Radiative losses due to pulse interactions in birefringent nonlinear optical fibers

Noel F. Smyth
Department of Mathematics and Statistics, The King's Buildings, University of Edinburgh, Edinburgh, Scotland EH9 3JZ, United Kingdom

William L. Kath
Department of Engineering Sciences and Applied Mathematics, 2145 Sheridan Road, McCormick School of Engineering and Applied Science, Northwestern University, Evanston, Illinois 60208-3125

(Received 13 October 2000; published 27 February 2001)

The transient evolution of two-polarization pulses in a birefringent nonlinear optical fiber, governed by coupled nonlinear Schrödinger (NLS) equations, is considered. The evolution is studied using a trial function consisting of coupled solitonlike pulses with varying parameters augmented by a radiative shelf in the Lagrangian formulation of the coupled equations, which yields ordinary differential equations for the pulse parameters. It is shown that including mass and momentum fluxes due to the radiative shelf is a requirement to obtain good agreement with full numerical solutions of the governing equations.

DOI: 10.1103/PhysRevE.63.036614 PACS number(s): 41.20.Jb, 42.65.Tg, 42.81.−i

I. INTRODUCTION

The use of solitons as the information bit in optical communication systems was proposed by Hasegawa and Tappert [1]. Solitons have a number of significant advantages as information carriers, the most important being the balancing of the inherent Kerr nonlinearity of the optical glass with linear chromatic dispersion, so that propagation occurs without change of form. Real optical fibers are birefringent, so that different polarizations travel with different velocities, which in the linear limit leads to signal splitting. Opposing this, however, the nonlinearity of the glass leads to cross-phase modulation which tends to hold the polarizations together. The propagation of a pulse through a birefringent fiber then depends on the relative importance of these two effects.

The propagation of optical solitons in a nonlinear, polarization maintaining birefringent optical fiber is described by the coupled nonlinear Schrödinger (CNLS) equations [2]

$$i\frac{\partial u}{\partial z}+\frac{1}{2}\frac{\partial^2 u}{\partial t^2}+(|u|^2+A|v|^2)u=0, \tag{1a}$$

$$i\frac{\partial v}{\partial z}+\frac{1}{2}\frac{\partial^2 v}{\partial t^2}+(|v|^2+A|u|^2)v=0. \tag{1b}$$

Here u and v are the complex amplitudes of the two orthogonally polarized modes propagating in the fiber and A is the cross-phase modulation (CPM) coefficient, where $0\leqslant A\leqslant 1$. The variable z is the distance down the fiber normalized by the dispersion length and t is the reduced time. The coupled NLS equations (1) have an exact inverse scattering solution for $A=0$, for which the system reduces to a pair of uncoupled NLS equations, and for $A=1$, for which the system is the Manakov equation. Therefore for $A=0$ and $A=1$ the solution of Eq. (1) is integrable and, in principle, fully known. For real fibers, however, $A=2/3$ and approximate or numerical methods must be used to describe pulse evolution.

The behavior of vector solitary wave solutions of the above equations has been investigated by a number of researchers, showing that only single-peaked, symmetric vector solitary waves are stable (see, e.g., [3,5,4,6]). The evolution of such solitonlike pulses has been explored using numerical and variational techniques [7–9]. In particular, the chirped Lagrangian method of Anderson [10] works remarkably well to describe the dynamics of these coupled pulses, at least for relatively short distances [11]. One of the main disadvantages of the variational method, however, is that dispersive radiation is not easily included. As the pulses propagate and collide, oscillations in their relative positions or amplitudes cause them to continually radiate. This radiation is particularly important when propagation over longer distances must be considered.

Kath and Smyth [12] developed an alternative hybrid variational method to calculate the effect of dispersive radiation on the evolution of pulse initial conditions for the NLS equation. The method provided a much improved approximation of the pulse evolution. In an independent study, Yang [9] linearized about a coupled vector soliton to calculate the radiation shed as a near-vector soliton initial condition evolves and showed the steady state of a vector soliton is reached by the loss of mass and energy via the shed dispersive radiation. Smyth and Worthy [13] extended the method of [12] to model a nonlinear twin-core fiber, which is governed by a system of two coupled NLS equations similar to the CNLS equations (1). It was found that including the dispersive radiation shed as the pulses evolve gives approximate solutions in much better agreement with full numerical solutions than those of previous work based on the chirp method of Anderson [10], which did not include this shed radiation.

Here we report on the extension and application of the hybrid method of [12] to the CNLS equations. As demonstrated by Yang [9], it will be shown that inclusion of the mass and momentum fluxes associated with the dispersive radiation shed as the pulses evolve is necessary in order to achieve good agreement with full numerical solutions of the coupled NLS equations.

II. APPROXIMATE EQUATIONS

The Lagrangian for the CNLS system (1) is

$$L=\frac{1}{2}i(u^*u_z-uu_z^*)-\frac{1}{2}|u_t|^2+\frac{1}{2}|u|^4+A|u|^2|v|^2 + \frac{1}{2}i(v^*v_z-vv_z^*)-\frac{1}{2}|v_t|^2+\frac{1}{2}|v|^4. \tag{2}$$

Here the asterisk denotes the complex conjugate and u, v, u^*, and v^* are taken to be separate variables when variations are taken. The key to the hybrid variational method is the choice of trial functions to substitute into the Lagrangian (2). In particular, it is critical that the effect of the dispersive radiation shed as the pulses evolve is included in the trial functions. Based upon work done for the NLS equation [12], the appropriate trial functions are

$$u=\eta_1\,\mathrm{sech}\,\frac{t-y_1}{w_1}e^{i\sigma_1+iV_1(t-y_1)}+ig_1e^{i\sigma_1+iV_1(t-y_1)}, \tag{3a}$$

$$v=\eta_2\,\mathrm{sech}\,\frac{t-y_2}{w_2}e^{i\sigma_2+iV_2(t-y_2)}+ig_2e^{i\sigma_2+iV_2(t-y_2)}. \tag{3b}$$

Here the parameters η_i, w_i, V_i, y_i, σ_i, and g_i, $i=1,2$, are functions of z. The first term in each expression is a varying solitonlike pulse, and the second term includes the effect of the dispersive radiation which lies in the vicinity of the pulse [12]. This radiation term is assumed to take the form of a flat shelf (since g_1 and g_2 have no t dependence) because both numerical solutions of the NLS equation and perturbed inverse scattering show that the radiation in the vicinity of the evolving pulse has little t variation. The physical reason for this is that the high-frequency radiation has the largest group velocity and so rapidly propagates away from the pulse, leaving low-frequency radiation only in its neighborhood. The trial functions (3) include the radiation in the vicinity of the pulse only, and the form of the dispersive radiation propagating away from the evolving pulses will be considered later. It is this radiation propagating away from the evolving pulses which causes them to evolve toward steady states. The shelf under the pulses u and v cannot be infinite, of course, since this would imply that they contain infinite mass. It is therefore assumed that the shelf for $u(v)$ is of length ℓ_1 (ℓ_2) centered about the pulse position $t=y_1$ (y_2).

Evolution equations for the pulse parameters in Eq. (3) are then obtained by substituting (3) into the Lagrangian (2) integrated over t from $t=-\infty$ to $t=\infty$,

$$\mathcal{L}=\int_{-\infty}^{\infty}L\,dt \tag{4}$$

(except for the terms describing the shelf, which only produce finite intervals). The result is

$$\mathcal{L}=-(\sigma_1'-V_1y_1')(2\eta_1^2w_1+\ell_1g_1^2)-\pi\eta_1w_1g_1'+\pi w_1g_1\eta_1' + \pi\eta_1g_1w_1'-\frac{1}{3}\frac{\eta_1^2}{w_1}-\frac{1}{2}\ell_1V_1^2g_1^2-V_1^2\eta_1^2w_1+\frac{2}{3}\eta_1^4w_1 + A\eta_1^2\eta_2^2I_1-(\sigma_2'-V_2y_2')(2\eta_2^2w_2+\ell_2g_2^2)-\pi\eta_2w_2g_2' + \pi w_2g_2\eta_2'+\pi\eta_2g_2w_2'-\frac{1}{3}\frac{\eta_2^2}{w_2}-\frac{1}{2}\ell_2V_2^2g_2^2-V_2^2\eta_2^2w_2 + \frac{2}{3}\eta_2^4w_2, \tag{5}$$

where the integral I_1 is given by

$$I_1=\int_{-\infty}^{\infty}\mathrm{sech}^2\,\theta_1\,\mathrm{sech}^2\,\theta_2\,dt,\quad \theta_1=\frac{t-y_1}{w_1},\quad \theta_2=\frac{t-y_2}{w_2}. \tag{6}$$

In deriving this approximate Lagrangian, it has been assumed that the amplitude of the dispersive radiation is much less than the pulse amplitudes, so that $|g_1|\ll\eta_1$ and $|g_2|\ll\eta_2$. Of the quadratic terms in g_1 and g_2 in the averaged Lagrangian, only those proportional to ℓ_1 and ℓ_2 have been retained. These terms are needed for mass conservation to be correct, while the others have little effect on the variational equations.

Taking variations of the averaged Lagrangian (5) with respect to each of the pulse parameters then gives the variational equations

$$\delta g_1:\quad \frac{d}{dz}(\eta_1w_1)=\frac{\ell_1g_1}{\pi}\left(\sigma_1'-\frac{1}{2}V_1y_1'\right), \tag{7a}$$

$$\delta\eta_1:\quad -4(\sigma_1'-V_1y_1')\eta_1w_1-2\pi w_1g_1'-\frac{2}{3}\frac{\eta_1}{w_1} -2V_1^2\eta_1w_1+\frac{8}{3}\eta_1^3w_1+2A\eta_1\eta_2^2I_1=0, \tag{7b}$$

$$\delta w_1:\quad -2(\sigma_1'-V_1y_1')\eta_1^2-2\pi\eta_1g_1'+\frac{1}{3}\frac{\eta_1^2}{w_1^2} -V_1^2\eta_1^2+\frac{2}{3}\eta_1^4+2A\frac{\eta_1^2\eta_2^2}{w_1^2}I_2=0, \tag{7c}$$

$$\delta V_1:\quad \frac{dy_1}{dz}=V_1, \tag{7d}$$

$$\delta\sigma_1:\quad \frac{d}{dz}(2\eta_1^2w_1+\ell_1g_1^2)=0, \tag{7e}$$

$$\delta y_1:\quad \frac{d}{dz}[(2\eta_1^2w_1+\ell_1g_1^2)V_1]=-\frac{2A\eta_1^2\eta_2^2}{w_2}I_3, \tag{7f}$$

plus similar equations due to variations in g_2, η_2, w_2, V_2, y_2, and σ_2. Also,

$$I_2=\int_{-\infty}^{\infty}(t-y_1)\,\mathrm{sech}^2\,\theta_1\,\mathrm{sech}^2\,\theta_2\tanh\theta_1\,dt \tag{8}$$

and

$$I_3=\int_{-\infty}^{\infty}\mathrm{sech}^2\,\theta_1\,\mathrm{sech}^2\,\theta_2\tanh\theta_2\,dt. \tag{9}$$

After some manipulation, the first four of the variational equations (7) become

$$\frac{d}{dz}(\eta_1 w_1)=\frac{\ell_1 g_1}{\pi}\left[\eta_1^2-\frac{1}{2}w_1^{-2}+A\frac{\eta_2^2}{w_1^2}(w_1I_1-I_2)\right], \tag{10a}$$

$$\frac{dg_1}{dz}=-\frac{2}{3\pi}\eta_1(\eta_1^2-w_1^{-2})-A\frac{\eta_1\eta_2^2}{\pi w_1^2}(w_1I_1-2I_2), \tag{10b}$$

$$\frac{d\sigma_1}{dz}-\frac{1}{2}V_1\frac{dy_1}{dz}=\eta_1^2-\frac{1}{2}w_1^{-2}+A\frac{\eta_2^2}{w_1^2}(w_1I_1-I_2), \tag{10c}$$

$$\frac{dy_1}{dz}=V_1. \tag{10d}$$

The last two variational equations, (7e) and (7f), are statements of the conservation of mass and momentum for u. From the NLS equation (1) one can show directly that the equations for conservation of u mass and momentum are

$$i\frac{\partial}{\partial z}(|u|^2)+\frac{1}{2}\frac{\partial}{\partial t}(u^*u_t-uu_t^*)=0, \tag{11a}$$

$$i\frac{\partial}{\partial z}(u^*u_t-uu_t^*)+\frac{1}{2}\frac{\partial}{\partial t}(u^*u_{tt}+uu_{tt}^*-2|u_t|^2+2|u|^4)=-2A|u|^2(v^*v_t+vv_t^*). \tag{11b}$$

Integrating Eq. (11a) from $t=-\infty$ to $t=\infty$ gives Eq. (7e) and integrating Eq. (11b) gives Eq. (7f).

In addition, the coupled NLS system (1) has the total-energy conservation equation

$$\begin{aligned}&i\frac{\partial}{\partial z}(|u_t|^2-|u|^4+|v_t|^2-|v|^4-2A|u|^2|v|^2)\\&\quad+\frac{1}{2}\frac{\partial}{\partial z}[u_t^*u_{tt}-u_tu_{tt}^*-2|u|^2(u^*u_t-uu_t^*)+v_t^*v_{tt}\\&\quad-v_tv_{tt}^*-2|v|^2(v^*v_t-vv_t^*)-2A|u|^2(v^*v_t-vv_t^*)\\&\quad-2A|v|^2(u^*u_t-uu_t^*)]=0.\end{aligned} \tag{12}$$

Integrating this from $t=-\infty$ to $t=\infty$ gives

$$\begin{aligned}\frac{dE}{dz}&=\frac{d}{dz}\left[\frac{2}{3}\frac{\eta_1^2}{w_1}+(2\eta_1^2w_1+\ell_1g_1^2)V_1^2-\frac{4}{3}\eta_1^4w_1+\frac{2}{3}\frac{\eta_2^2}{w_2}\right.\\&\quad\left.+(2\eta_2^2w_2+\ell_2g_2^2)V_2^2-\frac{4}{3}\eta_2^4w_2-2A\eta_1^2\eta_2^2I_1\right]\\&=0.\end{aligned} \tag{13}$$

This energy conservation result can be obtained directly by taking a combination of the variational equations (7). It should also be noted that the mass conservation equation (7e) can be obtained from a suitable combination of the energy conservation and other variational equations and is not independent.

The final system governing the evolution of the pulse parameters can therefore be taken to be the variational equations (10), the momentum conservation equation (11b), and the energy conservation equation (13), plus the similar variational and integrated momentum and energy conservation equations for the parameters of the v polarization. This makes a total of 12 equations for the 12 parameters.

For simplicity we will now restrict the discussion to the antisymmetric case for which $\eta_1=\eta_2$, $w_1=w_2$, $g_1=g_2$, $\sigma_1=\sigma_2$, $V_1=-V_2$, and $y_1=-y_2$. With these assumptions, the integrals I_j can be evaluated exactly and can easily be found to be

$$I_1=\frac{4w_1}{\sinh^2\zeta}[\zeta\coth\zeta-1], \tag{14a}$$

$$I_2=\frac{w_1^2}{\sinh^2\zeta}[\zeta\coth\zeta-1]-\frac{\zeta w_1^2}{\sinh^2\zeta}\times[3\coth\zeta+\zeta-3\zeta\coth^2\zeta], \tag{14b}$$

$$I_3=\frac{2w_1}{\sinh^2\zeta}[3\zeta\coth^2\zeta-3\coth\zeta-\zeta], \tag{14c}$$

where

$$\zeta=\frac{2y_1}{w_1}. \tag{15}$$

With this antisymmetry, the system of equations governing the evolution of the pulse then reduces to the six equations (10), (11b), and (13) for η_1, w_1, σ_1, V_1, y_1, and g_1.

Let us denote the fixed points of this system by $\eta_1=\hat{\eta}$, $w_1=\hat{w}$, $V_1=\hat{V}$, and $y_1=\hat{y}$. There are then two types of fixed points: that corresponding to a bound soliton, for which $\hat{\eta}\hat{w}=1/\sqrt{1+A}$ with $\hat{y}=\hat{V}=0$, and that corresponding to separated solitons in u and v, for which $\hat{\eta}\hat{w}=1$ with $y_1\to\infty$ as $t\to\infty$. This second type of fixed point is just a NLS soliton in each polarization.

These two fixed points indicate the two main types of behavior seen in this system. Consider the case where overlapped pulses start at the same t position in both the u and v polarizations. If the initial velocity difference is sufficiently

large, the pulses separate and become unbound as $z\to\infty$. If, however, the initial velocity is small enough, then the pulses remain bound and repeatedly oscillate about each other, shedding mass, momentum, and energy as $z\to\infty$.

From the energy conservation equation (13), the fixed point for a bound soliton is given by

$$\hat{\eta}^3=-\frac{3}{4}\frac{E_0}{\sqrt{1+A}}, \tag{16}$$

where E_0 is the initial value of the total energy. Similarly, the fixed point for separated, single polarization solitons is given by the solution of

$$\hat{\eta}^3-3\hat{V}^2\hat{\eta}+\frac{3}{4}E_0=0. \tag{17}$$

Unfortunately, $\hat{V}$ as $z\to\infty$ cannot be determined from the initial conditions via the conservation equations and must be determined from the full time-dependent solution of the approximate equations. If $E_0<0$, then the coupled steady state is stable and the pulses evolve toward the amplitude given by Eq. (16). If $E_0>0$, then the separated solitons form the stable steady state and the pulses evolve toward the amplitude given by Eq. (17).

The length of the shelf under the solitons ($\ell_1=\ell_2$ for the antisymmetric case considered here) is determined by the requirement that the frequency of oscillation in η_1 of the approximate equations approaches the soliton oscillation frequency as the steady state is approached [12]. From this requirement we obtain, on linearizing the approximate equations,

$$\ell_1=\frac{3\pi^2}{8\hat{\eta}\sqrt{1+A}},$$

$$\ell_1=\frac{3\pi^2}{8\hat{\eta}} \tag{18}$$

for the cases of a coupled soliton and separated solitons, respectively. The approximate equations (10), (11b), and (13) are not as yet complete, however, as the effect of the dispersive radiation propagating away from the evolving pulses has not been determined.

III. RADIATION LOSS

The effect of the radiation shed by the evolving pulses will now be determined in a similar manner to that used for the NLS equation [12]. It has been shown [12] that accounting for the mass and momentum loss due to radiation is sufficient to obtain a good approximation to the pulse behavior, and that energy loss can be neglected.

Since the shed radiation has small amplitude, it is governed by the linearized form of the coupled NLS equations (1),

$$i\frac{\partial u}{\partial z}+\frac{1}{2}\frac{\partial^2 u}{\partial t^2}=0, \tag{19a}$$

$$i\frac{\partial v}{\partial z}+\frac{1}{2}\frac{\partial^2 v}{\partial t^2}=0. \tag{19b}$$

These equations are basically the same as those governing the shed radiation for the NLS equation [12], but care must be taken because here the radiation is shed by accelerating pulses. This, of course, was not a relevant issue for the NLS equation, which has soliton solutions moving at constant velocity. To determine the effect of the acceleration, we shift (19a) to a frame of reference moving with the pulse using the transformations

$$\xi=t-\int_0^z V(\tau)d\tau,\quad u=U(\xi,z)e^{iV\xi+(1/2)i\int_0^z V^2(\tau)d\tau}, \tag{20}$$

so that

$$i\frac{\partial U}{\partial z}+\frac{1}{2}\frac{\partial^2 U}{\partial \xi^2}=\xi V_z U. \tag{21}$$

In general, this linear partial-differential equation for the dispersive radiation cannot be solved exactly. However, if it is assumed that $|V_z|$ is small, then to first order (21) is the same equation for the dispersive radiation as for the NLS equation [12].

We first consider the radiation shed to the right of the pulse. Keeping only the quadratic terms in the mass conservation equation (11a) for the coupled NLS equations (1) gives the mass conservation equation for the first of the linearized NLS equations (19a). Using the transformations (20), it can then be shown that the mass of the radiation shed to the right of the pulse is given by

$$\frac{d}{dz}\int_{y+\ell_1/2}^{\infty}|u|^2dt=\mathrm{Im}\,U^*U_\xi\big|_{\xi=\ell_1/2}. \tag{22}$$

Similarly, the mass radiated to the left of the pulse in the u polarization is found to be

$$\frac{d}{dz}\int_{-\infty}^{y-\ell_1/2}|u|^2dt=-\mathrm{Im}\,U^*U_\xi\big|_{\xi=-\ell_1/2}. \tag{23}$$

Adding together these two expressions to obtain the total mass loss by the radiating pulse and noting that it has been assumed that the shelf is flat in the neighborhood of the pulse, so that $|U(\ell_1/2,z)|=|U(-\ell_1/2,z)|$, we have

$$\frac{d}{dz}\int_{-\infty}^{\infty}|u|^2dt=\mathrm{Im}\,U^*U_\xi\big|_{\xi=\ell_1/2}-\mathrm{Im}\,U^*U_\xi\big|_{\xi=-\ell_1/2}. \tag{24}$$

With $|V_z|$ small, the Laplace transform solution of Eq. (21) for $V_z=0$ [12] gives

$$U_\xi(\ell_1/2,z) = -\sqrt{2}e^{-i\pi/4}\frac{d}{dz}\int_0^z \frac{r(\tau)}{\sqrt{\pi(z-\tau)}}d\tau, \qquad (25)$$

so that the mass shed from the pulse to the dispersive radiation is given by

$$\frac{d}{dz}\int_{-\infty}^{\infty}|u|^2dt = 2r\frac{d}{dz}\int_0^z \frac{r(\tau)}{\sqrt{\pi(z-\tau)}}d\tau. \qquad (26)$$

Here r is the height of the shelf, $r=|U(\ell_1/2,z)|=|u(y+\ell_1/2,z)|$.

In a similar manner, it can be shown that the total momentum in the dispersive radiation shed by the pulse in the u polarization is

$$i\frac{d}{dz}\int_{-\infty}^{\infty}(u^*u_t - uu_t^*)dt = [\mathrm{Re}(U^*U_{\xi\xi}) - |U_\xi|^2 - 2V\,\mathrm{Im}\,U^*U_\xi]\Big|_{\xi=-\ell_1/2}^{\xi=\ell_1/2}. \qquad (27)$$

With $|V_z|$ small, it can then be found on using Eq. (25) that the momentum lost to the dispersive radiation is [12]

$$i\frac{d}{dz}\int_{-\infty}^{\infty}(u^*u_t - uu_t^*)dt = -4Vr\frac{d}{dz}\int_0^z \frac{r(\tau)}{\sqrt{\pi(z-\tau)}}d\tau. \qquad (28)$$

Comparing the mass loss (26) with this momentum loss, it can be seen that the momentum loss is the result of the mass shed at velocity V into dispersive radiation. This is just an expression of the Galilean invariance of the mass and momentum conservation laws of the NLS equation.

As for the NLS equation [12], mass conservation can then be used to show that the height of the shelf is given by

$$r^2 = \frac{3\hat{\eta}\sqrt{1+A}}{8}\left[2\eta_1^2 w_1 - 2\frac{\hat{\eta}}{\sqrt{1+A}} + \ell_1 g_1^2\right] \qquad (29)$$

for the case when coupled solitons are the steady state and

$$r^2 = \frac{3\hat{\eta}}{8}[2\eta_1^2 w_1 - 2\hat{\eta} + \ell_1 g_1^2] \qquad (30)$$

for the case when separated solitons are the steady state. The mass loss (26) is now added to the equation for g_1 in Eq. (10) [12], so that this equation becomes

$$\frac{dg_1}{dz} = -\frac{2}{3\pi}\eta_1(\eta_1^2 - w_1^{-2}) - A\frac{\eta_1\eta_2^2}{\pi w_1^2}(w_1 I_1 - 2I_2) - 2\alpha g_1, \qquad (31)$$

where

$$\alpha = \frac{3\hat{\eta}\sqrt{1+A}}{8r}\frac{d}{dz}\int_0^z \frac{r(\tau)}{\sqrt{\pi(z-\tau)}}d\tau, \qquad (32a)$$

$$\alpha = \frac{3\hat{\eta}}{8r}\frac{d}{dz}\int_0^z \frac{r(\tau)}{\sqrt{\pi(z-\tau)}}d\tau \qquad (32b)$$

for the steady state of a coupled soliton or separated solitons, respectively. The momentum loss (28) is added to the momentum equation (11b), so that it becomes

$$\frac{d}{dz}[(2\eta_1^2 w_1 + \ell_1 g_1^2)V_1] = -\frac{2A\eta_1^2\eta_2^2}{w_2}I_3 - 2Vr\frac{d}{dz}\int_0^z \frac{r(\tau)}{\sqrt{\pi(z-\tau)}}d\tau. \qquad (33)$$

The full system of approximate equations governing the evolution of the pulses including mass and momentum loss to dispersive radiation is then Eqs. (10) with the equation for g_1 replaced by Eq. (31), Eq. (33), and Eq. (13).

In previous work [12], the integral in the mass loss term (26) was approximated using

$$\frac{d}{dz}\int_0^z \frac{r(\tau)}{\sqrt{\pi(z-\tau)}}d\tau \approx \frac{r^2}{r(0)\sqrt{\pi z}}, \qquad (34)$$

where $r(0)$ is the value of r at $z=0$. This approximation is appropriate for an initial value problem in which the pulse sheds a large amount of mass initially and then decays onto the steady state. In the present work, however, the pulses can oscillate about each other, with mass shed each time they pass through each other. To obtain accurate values of the mass integral in Eq. (26) in such oscillatory cases, the integral was evaluated numerically using the method of Miksis and Ting [14]. As the integral is singular at $z=\tau$, near this singular point the nonsingular part r of the integrand was approximated by a trapezoidal approximation and the singular part $1/\sqrt{\pi(z-\tau)}$ was evaluated exactly. Away from the singular point, the integral was evaluated using the trapezoidal rule.

The other complication occurs for the separated soliton fixed point because the steady velocity $\hat{V}$ is not determined by the conservation equations. This means that the fixed point $\hat{\eta}$ cannot be determined from Eq. (17), so that the radiation damping given by Eq. (32b) cannot be evaluated. To overcome this, the steady velocity $\hat{V}$ was found using a shooting method. For the initial iteration, the instantaneous value of V_1 at each space step was used to estimate $\hat{V}$ and the fixed point $\hat{\eta}$ was then estimated at each space step by

$$\hat{\eta} = \left[3V_1^2\eta_1 - \frac{3}{4}E_0\right]^{1/3}, \qquad (35)$$

which is a single Picard iteration on Eq. (17). When the solution had settled to a steady state, the steady value of V_1 was used as a new approximation for $\hat{V}$ and a new approximation to $\hat{\eta}$ was then found by solving Eq. (17). This process was repeated until the iterates for $\hat{V}$ converged. This shoot-

ing method to determine $\hat{V}$ worked quite well unless the initial conditions were such that little radiation was produced (for instance, when η_0 was small). In such cases, the initial iterates could have $r(0)<0$ (and small), which is unphysical and the iteration would not converge. In this case, the simplest fix was to ignore the mass loss, since the shed radiation was very small, in which case the iterations converged rapidly.

IV. RESULTS

In this section solutions of the approximate equations derived in Secs. II and III will be compared with full numerical solutions of the coupled NLS equations (1). The numerical method used to solve the coupled NLS equations was a pseudospectral method based on that of Fornberg and Whitham [15] for the Korteweg–de Vries equation. The t derivatives in the coupled NLS equations (1) were evaluated using fast Fourier transforms (FFT's) and then the equations were propagated forward in space z using a fourth-order Runge-Kutta scheme in Fourier space. The approximate evolution equations were numerically integrated using a fourth-order Runge-Kutta scheme.

As a first test we compared the numerical solution of the full and approximate equations for the case of separating pulses. For this test, we used the initial conditions $\eta_1=\eta_0$, $w_1=1/\eta_0$, $V_1=1.0$, $y_1=0.0$ (with $g_1=0.0$ so that no radiation is present initially), with $A=2/3$, which corresponds to antisymmetric polarizations started with a relative velocity difference of 2. For this initial condition and η_0 sufficiently small, the solution evolves to a pair of separated solitons with $\eta_1=1/w_1$ as $z\to\infty$. Due to the cross-phase modulation, the velocity V_1 changes (slows) by an amount δV. Since the steady velocity $\hat{V}$ cannot be determined from the conservation equations, the shooting method outlined in Sec. III was used to determine the steady state. Also, since the pulses' positions do not oscillate about each other in this case, the approximation (34) was used to evaluate the integral in Eq. (26). Using this approximation together with the shooting method to determine the fixed point, however, gives $r(0)=0$ for the initial iterate of the shooting method. To overcome this initial singularity, the mass loss given by the integral (34) in Eqs. (31) and (33) was ignored for the first iteration of the shooting method. However, for all subsequent iterations, $r(0)\neq 0$ and so the mass loss terms were included for all subsequent iterations.

Figure 1 shows a comparison between δV as a function of the initial amplitude η_0 as given by the full numerical solution of the coupled NLS equations (1), by the solution of the present approximate equations, and by the chirped variational equations [7,11]. It can be seen that both approximate methods give excellent agreement with the full numerical solution until about $\eta_0=1$. After this point, they start to diverge somewhat from the numerical results, but are still in good agreement with the numerical solution. The velocity change δV as given by the chirp equations is in slightly better agreement with the numerical results than that given by the present equations as the cutoff is approached. Wang

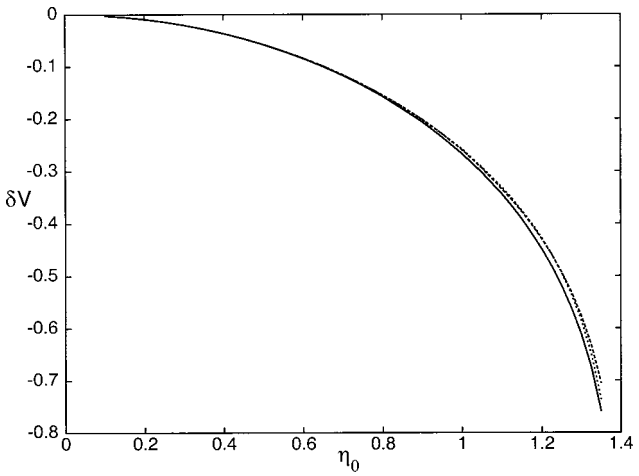

FIG. 1. Comparison between the velocity δV as given by the full numerical solution (—), the present approximation (– – –), and the chirped variational approximation (- - -). The initial values are $\eta_1=\eta_0$, $w_1=1/\eta_0$, $V_1=1.0$, and $y_1=0$ with $A=2/3$.

et al. [11] used various approximate methods to determine δV and compared these approximate values with full numerical solutions of the coupled NLS equations (1). They found that the best comparison was obtained using the chirped variational method [7]. We note that this chirp method includes an approximation to the radiation moving with the evolving pulses, but does not include the radiation shed by the pulses.

While the chirped variational method [7] gives good agreement for the velocities of the pulses, it does not give good agreement for the other pulse parameters. Figure 2 shows the space evolution of the amplitude of the pulse u for the initial conditions $\eta_1=1.15$, $w_1=1/\eta_1$, $V_1=1$, and $y_1=0$ with $A=2/3$. Although the values of δV obtained by the two approximate methods for this initial condition are very close, it can be seen that the present approximate equations give markedly improved accuracy for the magnitude of the pulse amplitude oscillation. The chirped variational equations predict an amplitude oscillation with constant amplitude. This, of course, is due to the chirped method not taking any account of the radiation shed by the evolving pulses.

The reason why the approximate equations break down as the cutoff in V_1 is approached is apparent if the numerical solution is examined for values of η_0 near the cutoff. From Fig. 3 it can be seen that for sufficiently large η_0 the input pulse splits and a shadow pulse (the smaller one in the figure) follows the pulse in the other polarization. This shadow pulse is dragged along and continues to interact for a very large time, so that a steady state is only slowly approached. Neither the chirped variational method [7] nor the present approximate method take full account of this shadow pulse, so it is not surprising that both approximate solutions break down when this pulse splitting occurs. What is surprising, however, is that quite accurate values of δV are predicted even when the pulse splitting begins to occur. Theoretically, it is possible to extend the approximate method to take ac-

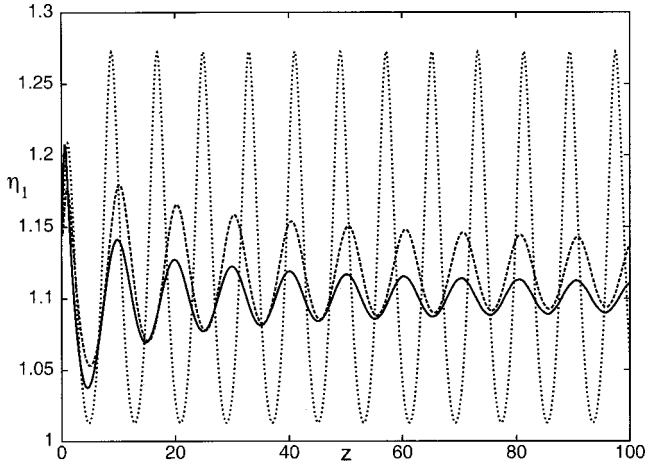

FIG. 2. The amplitude of the pulse u as a function of z for the initial conditions $\eta_1=1.15$, $w_1=1/\eta_1$, $V_1=1$, and $y_1=0$ with $A=2/3$. Full numerical solution, — ; solution of present approximate equations, – – –; solution of chirped variational equations, - - -.

count of the split pulse by adding a second pulse to the trial function (3). Doing this, however, vastly increases the complexity of the resulting equations due to the cross-terms resulting from the nonlinear terms $(|u|^2+A|v|^2)u$ and $(|v|^2+A|u|^2)v$ in the coupled NLS equations.

The present approximate method accounts for this second pulse to a certain extent, as can be seen from the following argument. From the symmetric location of the shadow pulse in Fig. 3, it can be seen that the shadow pulse is locked onto the main pulse in the v polarization. Hence it will have the same width as this v pulse. The mass in the main u pulse at a given time is $M_1=2\eta_1^2 w_1+\ell_1 g_1^2$. From the solution of the approximate equations, it is found that at $z=80$, $w_1=0.787\,02$, and $M_1=2.5082$. Let us assume that all the mass shed by the main pulse has gone into forming the shadow pulse. Then assuming that the shadow pulse has the soliton-like profile $\tilde{\eta}\,\mathrm{sech}(x+y_1)/w_1$ and noting that the initial mass is $M_1=2.65$, we find that $\tilde{\eta}=0.3001$. This amplitude is in

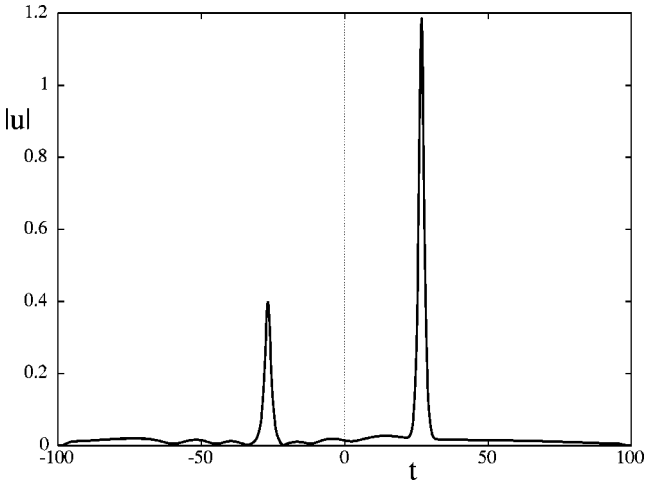

FIG. 3. Numerical solution at $z=80$ for the initial values $\eta_1=1.325$, $w_1=1/\eta_1$, $V_1=1.0$, and $y_1=0.0$ with $A=2/3$.

reasonable agreement with the amplitude seen in Fig. 3. It is then clear that the shadow pulse is being formed from the mass shed by the main pulse. The present approximate method can account for the amount of mass shed, but it cannot account for the accumulation of this mass in the vicinity of the main part of the v pulse.

We now consider a case in which the pulses evolve to the coupled solitary wave steady state [7]. We take the initial values $\eta_1=1.0$, $w_1=1/\sqrt{1+A}$, $V_1=0.1$, $y_1=0.0$ with $A=0.1$ (and $g_1=0.0$ so that no radiation is present initially). The evolution of the pulse amplitude η_1 is shown in Fig. 4(a). It can be seen that the comparison between the approximate and numerical solutions is very good. There is a beating effect apparent in the numerical solution which is not fully mirrored in the approximate solution, but otherwise the comparison is excellent. The importance of the shed dispersive radiation can be seen from the next figure, Fig. 4(b). This figure shows the pulse amplitude η_1 as a function of z for the

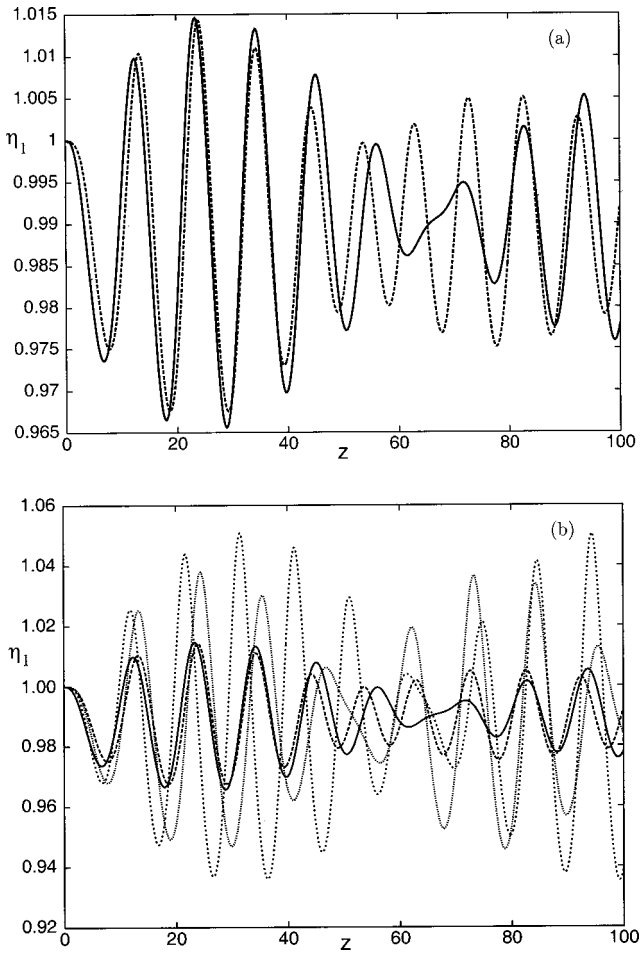

FIG. 4. Comparison between the full numerical solution of the coupled NLS equations (1) and the solutions of the approximate equations, showing evolution of η_1 as a function of z. The initial values are $\eta_1=1.0$, $w_1=1/(\eta_1\sqrt{1+A})$, $V_1=0.1$, and $y_1=0.0$ with $A=0.1$. (a) Full numerical solution, —; solution of present approximate equations, – – – . (b) Full numerical solution, —; solution of present approximate equations, – – –; solution of chirped variational equations, - - -; solution of present approximate equations without radiative damping, · · · .

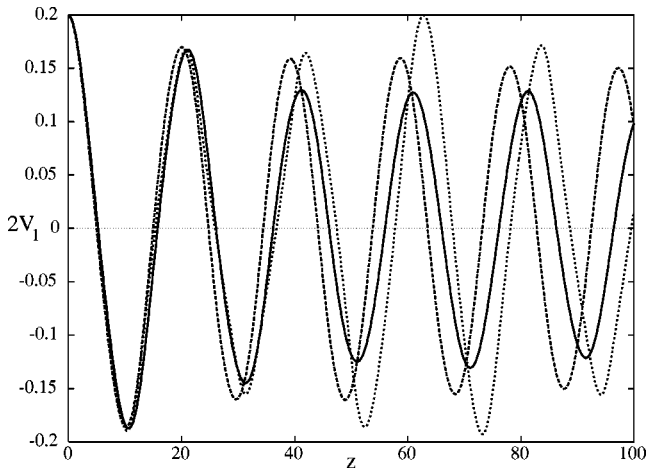

FIG. 5. Comparison between the full numerical solution of the coupled NLS equations (1) and the solutions of the approximate equations, showing evolution of $2V_1$ as a function of z. The initial values are as for Fig. 4. Full numerical solution, —; solution of present approximate equations, – – – ; solution of chirped variational equations, - - - .

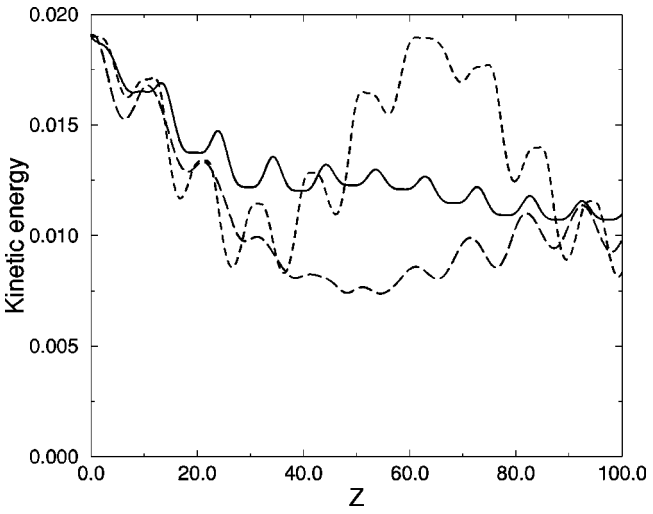

FIG. 6. Pulse kinetic energy as a function of z. Numerical solution, —; present approximate equations with damping, – – –; solution of chirped variational equations, - - -.

same parameters as Fig. 4(a) as given by the full numerical solution, the chirped variational approximation [7], and the present approximate equations with and without radiation damping. It can be seen that both the chirped equations and the present approximate equations without taking radiation into account give large overestimates of the pulse amplitude oscillations. It is therefore seen that to obtain a good approximation of the pulse evolution, the shed dispersive radiation must be included.

In Fig. 5 the relative velocity $2V_1$ of the pulses as a function of z is shown for the same initial conditions as in Fig. 4(a). Shown in the figure are results from the full numerical solution, the present approximate method, and the chirped variational method [7]. It can be seen that there is again good agreement between the numerical solution and the present approximate solution, with the damping of the approximate solution being slightly less than the actual damping. The greater velocity damping present in the numerical solution is in accord with the results shown in Fig. 1 and results from the momentum shed by the pulses being greater than that predicted by the approximate equations. The velocity as predicted by the chirp equations is in good agreement with the numerical solution in the initial stages of the evolution. However, since there is no damping present in the chirp equations, the velocity oscillates in a quasiperiodic fashion.

The importance of the shed dispersive radiation can also be seen in Fig. 6. Here, the approximate ODE equations have been used to define an effective ''kinetic'' energy for the motion of the centers of the two polarizations [7]. (The other main degree of freedom is then thought of as an ''internal'' bound up on oscillations of the pulse amplitude and width.) Using guidance from the ODE equations, one can define an effective pulse kinetic energy

$$E_{\mathrm{kin}}=A\int_{-\infty}^{\infty}|u|^4dt-A\int_{-\infty}^{\infty}|u|^2|v|^2dt+\left[\frac{\left(\int_{-\infty}^{\infty}\mathrm{Im}(u^*u_t)dt\right)^2}{\int_{-\infty}^{\infty}|u|^2dt}\right].$$

Figure 6 shows this effective kinetic energy as a function of distance z for the full CNLS numerics, the chirped variational method, and the present method including dispersive radiation. While neither ODE approximation is in perfect quantitative agreement with the full numerics, the approximation including dispersive damping does a better job of predicting the qualitative behavior of the pulse energy. In particular, since the chirped variational equations include no effects due to dispersive radiation [7], they produce a pulse energy that is almost periodic with distance.

V. CONCLUSIONS

In summary, we have used a hybrid variational method that includes the effects of dispersive radiation to describe the transient evolution of coupled pulses in a birefringent nonlinear optical fiber. It is shown that the inclusion of mass and momentum fluxes due to the dispersive radiation is a requirement for obtaining good agreement between approximate and full numerical solutions of the governing equations.

ACKNOWLEDGMENTS

This work was supported in part by grants from NATO (No. 920557), the Air Force Office of Scientific Research (Air Force Materials Command, USAF under Grant No. F49620-99-1-0016), and the National Science Foundation (Grant No. DMS-09804602).

[1] A. Hasegawa and F. Tappert, Appl. Phys. Lett. **23**, 142 (1973).
[2] C. R. Menyuk, IEEE J. Quantum Electron. **QE-23**, 174 (1987).
[3] V. K. Mesentsev and S. K. Turitsyn, Opt. Lett. **17**, 1497 (1992).
[4] M. Haelterman and A. P. Sheppard, Phys. Lett. A **194**, 191 (1994).
[5] Y. Silberberg and Y. Barad, Opt. Lett. **20**, 246 (1995).
[6] J. Yang and D. J. Benney, Stud. Appl. Math. **96**, 111 (1996).
[7] T. Ueda and W. L. Kath, Phys. Rev. A **42**, 563 (1990).
[8] D. J. Kaup, B. A. Malomed, and R. S. Tasgal, Phys. Rev. E **48**, 3049 (1993).
[9] J. Yang, Stud. Appl. Math. **98**, 61 (1997).
[10] D. Anderson, Phys. Rev. A **27**, 3135 (1983).
[11] Q. Wang, P. K. A. Wai, C.-J. Chen, and C. R. Menyuk, J. Opt. Soc. Am. B **10**, 2030 (1993).
[12] W. L. Kath and N. F. Smyth, Phys. Rev. E **51**, 1484 (1995).
[13] N. F. Smyth and A. L. Worthy, J. Opt. Soc. Am. B **14**, 2610 (1997).
[14] M. J. Miksis and L. Ting, Comput. Fluids **16**, 327 (1988).
[15] B. Fornberg and G. B. Whitham, Philos. Trans. R. Soc. London, Ser. A **289**, 373 (1978).